FEBS Letters 471 (2000) 128–132 FEBS 23515

Interaction of fMet-tRNA^{fMet} with the C-terminal domain of translational initiation factor IF2 from *Bacillus stearothermophilus*

Christoph Krafft[a,1,2], Annette Diehl[a,1], Stefan Laettig[a], Joachim Behlke[a], Udo Heinemann[a,b], Cynthia L. Pon[c], Claudio O. Gualerzi[c], Heinz Welfle[a,*]

[a] *Max-Delbrück-Centrum für Molekulare Medizin, D-13092 Berlin, Germany*
[b] *Institut für Kristallographie, Freie Universität, D-14195 Berlin, Germany*
[c] *Laboratory of Genetics, Department of Biology MCA, University of Camerino, 62032 Camerino (MC), Italy*

Received 14 February 2000

Edited by Vladimir Skulachev

Abstract Analytical ultracentrifugation studies indicated that the C-terminal domains of IF2 comprising amino acid residues 520–741 (IF2 C) and 632–741 (IF2 C-2) bind fMet-tRNA with similar affinities (K_d at 25°C equal to 0.27 and 0.23 μM, respectively). Complex formation between fMet-tRNA^{fMet} and IF2 C or IF2 C-2 is accompanied by barely detectable spectral changes as demonstrated by a comparison of the Raman spectra of the complexes with the calculated sum of the spectra of the individual components. These results and the temperature dependence of the K_d of the protein–RNA complexes indicate that complex formation is not accompanied by obvious conformational changes of the components, and possibly depends on a rather small binding site comprising only a few interacting residues of both components.

Key words: Protein synthesis; fMet-tRNA binding; Analytical ultracentrifugation; Raman spectroscopy

1. Introduction

Initiation of protein biosynthesis requires the correct positioning of charged initiator tRNA, fMet-tRNA^{fMet}, in the ribosomal P-site of the mRNA-programmed 70S ribosomes. This is accomplished by translation initiation factor IF2, which interacts with GTP and 50S ribosomal subunits through its central 40 kDa G domain and with fMet-tRNA through its C-terminal domain (IF2 C) [1–5]. Knowledge about the molecular nature of this interaction is particularly relevant in light of the vital importance of this interaction which represents a new target for a new class of specific antibacterial agents.

Recently we have shown that the fMet-tRNA binding site is localised in a small C-terminal sub-domain of IF2 C (IF2 C-2) [6–8]. Because of their small size IF2 C and IF2 C-2 from *Bacillus stearothermophilus*, obtained by expression in *Escherichia coli* [4,8], are useful models to study the interaction of IF2 with fMet-tRNA.

Here we present data on complex formation between fMet-tRNA^{fMet} and IF2 C and IF2 C-2. Analytical ultracentrifugation was used to determine the dissociation constants of the complexes at various temperatures, while Raman spectroscopy was used to investigate the nature of specific interactions and possible conformational changes in the protein or RNA which might occur during complex formation.

2. Materials and methods

2.1. Chemicals

All chemicals were of analytical grade unless indicated otherwise. The formyl donor N^{10}-formyltetrahydrofolate for the transformylation reaction was prepared according to the published procedure [9].

2.2. Proteins and tRNA

IF2 C and IF2 C-2 from *B. stearothermophilus* were prepared and purified according to [3] and [8], respectively. tRNA^{fMet} was supplied by Subriden (Seattle, WA, USA).

2.3. Aminoacylation and formylation of tRNA^{fMet}

The reaction mixture contained 30 μM tRNA^{fMet} in 20 mM imidazole–HCl pH 7.5, 150 mM NH_4Cl, 4 mM $MgCl_2$, 10 mM β-mercaptoethanol, 2 mM ATP, 42 μM methionine and 1 mM N^{10}-formyltetrahydrofolate. After 15 min incubation at 37°C with *E. coli* methionyl-tRNA synthetase [10], *E. coli* formyltransferase [11] was added and incubation continued for an additional 5 min. The resulting fMet-tRNA^{fMet} was purified by phenol extraction, ethanol precipitation and hydrophobic interaction chromatography [12]. Immediately after elution, the fractions containing fMet-tRNA^{fMet} were pooled, the pH adjusted to 6 and the sample dialysed against 20 mM K-acetate buffer, pH 5.4, 0.4 mM EDTA, 20 mM β-mercaptoethanol.

2.4. Sample preparation

Proteins, fMet-tRNA^{fMet} and tRNA^{fMet} were concentrated in Ultrafree devices (Millipore) with a 5 kDa cut-off. Charged and uncharged tRNA were transferred into 10 mM HEPES, pH 5.6, 5 mM $MgCl_2$, 300 mM NH_4Cl. RNA concentrations were determined spectrophotometrically at 260 nm using an absorption coefficient of 606 060 M^{-1} cm^{-1} (tRNA^{fMet}, M_r 26 250; fMet-tRNA^{fMet}, M_r 26 410). The IF2 domains were transferred into 10 mM HEPES–KOH, pH 7.2, 5 mM $MgCl_2$, 300 mM NH_4Cl.

Protein concentrations were determined at 280 nm using absorption coefficients of 10 672 M^{-1} cm^{-1} for IF2 C (M_r 24 540) and 7800 $M^{-1}cm^{-1}$ for IF2 C-2 (M_r 12 890).

2.5. Gel electrophoresis

Complex formation and stability were checked by non-denaturing PAGE on 8% gels before and after Raman spectroscopy applying 0.5 μl of each sample. 20 mM MOPS, pH 7.5, was used as gel and electrophoresis buffer. Protein, tRNA and complex were detected by silver staining [13].

2.6. Analytical ultracentrifugation

Sedimentation equilibrium experiments were carried out using an

*Corresponding author. Fax: (49)-30-94062840.
E-mail: welfle@mdc-berlin.de

[1] These authors have contributed equally to this work.
[2] Present address: School of Biological Sciences, Division of Cell Biology and Biophysics, University of Missouri-Kansas City, Kansas City, MO 64110, USA.

PII: S0014-5793(00)01377-6

XL-A type analytical ultracentrifuge (Beckman) equipped with UV absorbance optics. Sample concentrations were adjusted such that extinctions were between 0.2 and 0.8 (path length 1.2 cm). Sedimentation equilibrium was analysed using externally loaded six-channel centrepieces of 12 mm optical path usually filled with 70–80 μl of liquid. This cell type allows the analysis of three solvent solution pairs [14]. Three of these cells were employed to simultaneously analyse different samples (free protein, free tRNA or mixtures of both). Sedimentation equilibrium was reached after 2 h of overspeed of 28 000 rpm, followed by an equilibrium speed of 24 000 rpm for about 24 h [15]. The radial absorbances of each compartment were scanned at three different wavelengths, 280 or 230 nm for protein absorbance and 260 nm for RNA absorbance; radial concentration distributions were calculated using the molar absorption coefficients given above.

Molecular masses were calculated from the sets of three radial absorbance distribution curves using our computer program Polymole [16]. The partial specific volume was calculated from the nucleotide and amino acid composition (fMet-tRNA^{fMet}, 0.55 ml/g; IF2 C, 0.7475 ml/g; IF2 C-2, 0.7382 ml/g). The association reactions were analysed by Polymole [16] in terms of the number of possible binding steps and the dissociation constant.

2.7. Calculation of free energy ΔG, enthalpy change ΔH, and entropy change ΔS of complex formation

The enthalpy change ΔH of complex formation was calculated from the slope of the van't Hoff plot ($\ln K$ versus $1/T$) of the temperature dependence of K_d. ΔG was calculated from the dissociation constant K_d and the entropy change ΔS was obtained from ΔG and ΔH.

2.8. Raman spectroscopy

Raman spectra were measured as described earlier in more detail [17] with the spectrometer T64000 (Jobin Yvon, France). Home-made cuvettes consisting of cylindrical quartz bodies with plane quartz bottoms and Teflon stoppers were filled with approximately 12 μl sample solutions. The samples were excited with the 488 nm line of an Innova 90 argon laser (COHERENT, Santa Clara, CA, USA), and the Raman scattering was collected in a 90° setup. The measurements were repeated with 514.5 nm excitation. Interference filters were used to eliminate plasma lines. The excitation energy at the sample was about 150 mW. Rayleigh scattering was separated by Notch filters, and Raman scattering was recorded with a liquid nitrogen-cooled CCD detector. Temperature was held constant at 23°C. To enhance the signal to noise ratio, 10 spectral scans of 20 s each at four spectrometer positions were averaged for the region 600–1720 cm^{-1}.

Raman data analysis, including buffer subtraction and background correction, was performed with the software package Spectramax (Jobin Yvon) and GRAMS/32 (Galactic Instruments Corp.). Solution spectra were corrected by subtraction of the buffer spectrum. A slight fluorescence background was approximated by a polynomial curve.

For the calculation of the sum spectrum the single component spectra were normalised in such a way that intensity differences with regard to the complex spectrum are minimal in the 990–1010 cm^{-1} and 1080–1120 cm^{-1} regions. These regions were selected for the normalisation procedure because the intensities of their prominent Raman bands are supposed not to change with complex formation. The band at 1003 cm^{-1} is assigned to breathing vibration of the phenyl ring which is insensitive to protein conformation [18]. The band at 1100 cm^{-1} is assigned to the stretching vibration of the phosphate dioxy group which is insensitive to protein–RNA complex formation [19].

3. Results and discussion

3.1. Gel shift experiments

Previous reports [20,21] have demonstrated that fMet-tRNA^{fMet}, but not uncharged tRNA^{fMet}, forms complexes with IF2. Preliminary gel shift experiments, carried out in the course of this work (not shown), extended this premise as far as IF2 C and IF2 C-2 are concerned demonstrating that both proteins form stable complexes with fMet-tRNA^{fMet}, while neither binds to uncharged tRNA^{fMet}. Gel shift experiments were then routinely performed to assess the formation of the complexes and to demonstrate that they remain stable over an extended period of time (e.g. for several days after the Raman measurements).

3.2. Molecular mass determinations

The molecular masses of IF2 C, IF2 C-2 and fMet-tRNA^{fMet} were determined by sedimentation equilibrium centrifugation and fitting the radical concentration distributions using the program Polymole [16]. All samples were found to be in the monomeric state since the experimentally determined masses are close to those derived from the nucleotide or amino acid sequence of the molecules. The masses determined were: fMet-tRNA^{fMet}, 26 740 ± 377 Da; IF2 C, 24 510 ± 941 Da; IF2 C-2, 13 388 ± 857 Da.

3.3. Analytical ultracentrifugation studies of complex formation

IF2 C or IF2 C-2 was mixed at different molar ratios with fMet-tRNA^{fMet} and centrifuged at 10, 20, 25, 30, and 37°C. Control experiments were performed with uncharged tRNA^{fMet}. Radial concentration distribution curves were calculated from the radial absorbances. Deconvolution considering mass conservation and optimal fit by Polymole [16] yields a small portion of free reactants (not shown) and predominantly 1:1 complexes for both IF2 C·fMet-tRNA^{fMet} and IF2 C-2·fMet-tRNA^{fMet} interactions. The dissociation constants, K_d, were calculated for each temperature from these data (see below).

The interaction of fMet-tRNA^{fMet} with IF2 C and IF2 C-2 was also studied over a broader range of protein–RNA ratios. Independent of the ratio, IF2 C and IF2 C-2 were found to form 1:1 complexes with fMet-tRNA^{fMet} with $K_d = 26$ nM and 20 nM, respectively, at 10°C (Fig. 1A). When substituting fMet-tRNA^{fMet} by uncharged tRNA^{fMet} only a very small portion of 1:1 complex was observed indicating an at least two orders of magnitude lower binding constant.

The temperature dependence of the dissociation constants calculated from the above data is shown in Fig. 1B as a van't Hoff plot ($\ln K_d$ versus $1/T$). Between 10 and 37°C, the K_d values were found to range from 25 nM to 1.4 μM and their values as well as their temperature dependences were found to be very similar for the complexes formed by fMet-tRNA^{fMet} with IF2 C and IF2 C-2. The free energies ΔG corresponding to the dissociation constants determined between 10 and 37°C range from −9.9 to −8.3 kcal mol^{-1}.

Experiments of fMet-tRNA^{fMet} protection at 37°C yielded an apparent K_d value of 1.8 μM for the complexes of fMet-tRNA^{fMet} with IF2, IF2 C and IF2 C-2 [8,22]. Gel shift experiments described earlier, on the other hand, established an upper limit of 0.2 μM for the dissociation constant of the complex of fMet-tRNA^{fMet} and IF2 C at room temperature [5]. Considering the temperature dependence of K_d observed here, these values agree reasonably well with our estimates at 30°C which gave K_d values of 0.59 μM and 0.81 μM for IF2 C and IF2 C-2, respectively.

3.4. Changes of enthalpy (ΔH) and entropy (ΔS) of complex formation

As seen in Fig. 1B, the temperature dependence of $\ln K$ was found to be linear over the whole temperature range examined. Linearity of the van't Hoff plot is expected for reactions with a heat capacity change ΔC_p close to zero. For such cases, according to the van't Hoff equation $d\ln K/d(1/T) = -\Delta H°/$

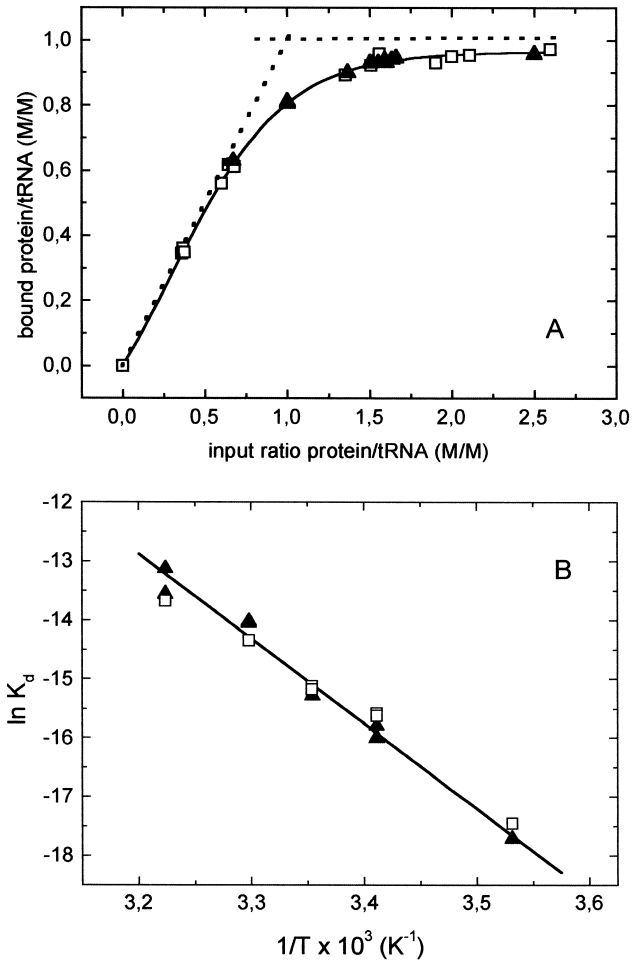

Fig. 1. Analytical ultracentrifugation of fMet-tRNA^{fMet}, IF2 C and IF2 C-2 and their complexes. A: Binding plot of the fMet-tRNA^{fMet}·IF2 C (□) and fMet-tRNA^{fMet}·IF2 C-2 (▲) interactions at 10°C; the fMet-tRNA^{fMet} concentration was kept constant at 0.50 μM while the protein concentrations were varied to give the input protein/RNA molar ratios indicated on the abscissa. A dissociation constant $K_d = 20 \pm 9$ nM was deduced from this plot. B: Van't Hoff plot of the temperature dependence of the dissociation constants ($\ln K_d$ vs. $1/T$) of the complexes of fMet-tRNA^{fMet} with IF2 C (□) and IF C-2 (▲). The line shows the linear fit through the experimental data.

RT, the enthalpy change ΔH can be obtained from the slope of the van't Hoff plot. Thus, the data shown in Fig. 1B yielded an enthalpy change $\Delta H = -29.4$ kcal mol^{-1}, and from this a free energy change $\Delta G_{25°C} = -9.0$ kcal mol^{-1} and an entropy change $\Delta S = -68$ cal mol^{-1} K^{-1}.

Large ΔC_p values, typically observed when binding of proteins to DNA is associated with conformational changes of the ligands, are associated with large temperature dependence of ΔH and ΔS and with a non-linear temperature dependence of ΔG (or $\ln K$). Thus, as mentioned above, a reasonable explanation for the linear dependence of $\ln K$ versus $1/T$ over an extended temperature range observed with IF2 C·fMet-tRNA^{fMet} and IF2 C-2·fMet-tRNA^{fMet} could be a small ΔC_p. This situation is typical of systems where the components do not undergo large conformational changes and behave like rigid bodies [23]. The Raman spectroscopic studies described below are consistent with this explanation indicating that the conformation of neither IF2 C, IF2 C-2 nor fMet-tRNA^{fMet} is noticeably changed upon complex formation. Of course, the experimental determination of ΔC_p (e.g. from isothermal titration experiments of the complex formation at different temperatures) would be necessary to verify this premise.

3.5. *Characterisation of IF2 C-2, fMet-tRNA^{fMet} and tRNA^{fMet} by Raman spectroscopy*

The Raman spectrum of IF2 C-2 (Fig. 2A, line 2) is significantly different from that of IF2 C [6]. The spectral differences are partly due to differences in their aromatic amino acid content and also to differences in their secondary structures. A very low content of α-helix in IF2 C-2 is indicated by the

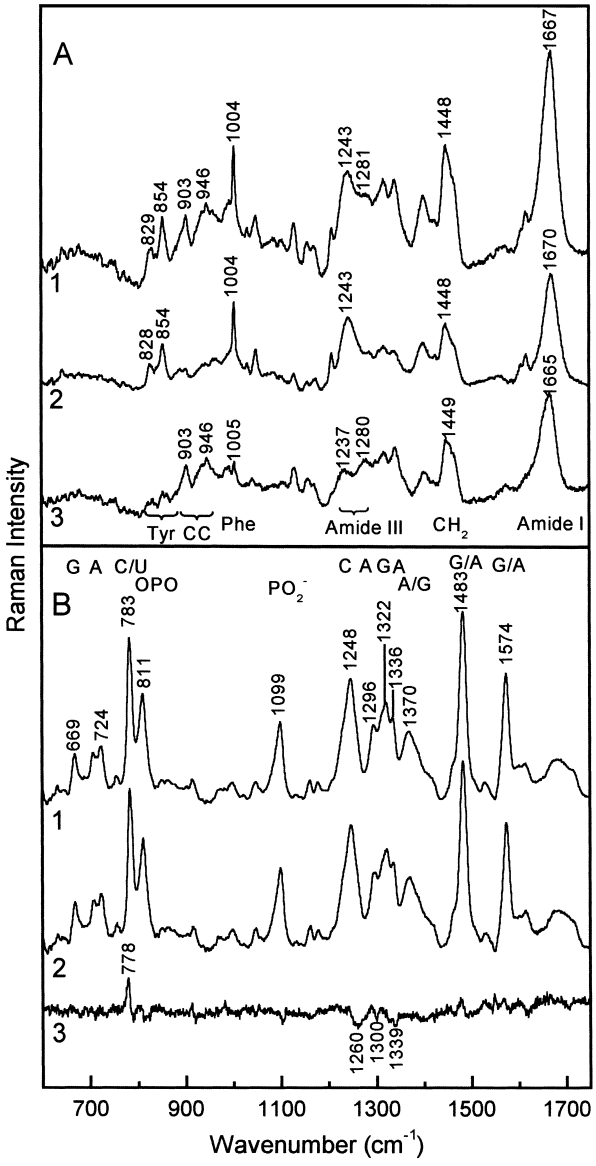

Fig. 2. Raman spectra of IF2 C, IF2 C-2 and fMet-tRNA^{fMet}. A: Spectra of IF2 C (line 1), IF2 C-2 (line 2) and difference spectrum IF2 C minus IF2 C-2 (line 3). B: Spectra of fMet-tRNA^{fMet} (line 1), tRNA^{fMet} (line 2) and three times enlarged difference spectrum fMet-tRNA^{fMet} minus tRNA^{fMet} (line 3). All spectra were measured with 488 nm excitation and corrected for the contribution of the buffer. Assignments of major peaks were made according to [25].

amide III band at 1243 cm^{-1}, amide I at 1670 cm^{-1}, and weak bands of C–C stretching vibrations at 902 and 946 cm^{-1}. This is in full agreement with the β-barrel structure of sub-domain IF2 C-2 which has recently been elucidated by multinuclear NMR spectroscopy [24]. No structural information is available yet concerning the N-terminal sub-domain of IF2 C (IF2 C-1). If the difference spectrum (IF2 C minus IF2 C-2; Fig. 2A, line 3) roughly corresponds to the spectrum of IF2 C-1, the Raman data indicate that this sub-domain has a rather high content of α-helical structure (strong and weak amide III bands at 1280 and 1237 cm^{-1}, respectively; amide I band at 1665 cm^{-1}, intensive bands at 903 and 946 cm^{-1}). Furthermore, the weak intensities at 830 and 850 cm^{-1} are consistent with the presence of only one Tyr residue in IF2 C-1 whereas IF2 C-2 contains six Tyr.

The Raman spectra of charged and uncharged $tRNA^{fMet}$ (Fig. 2B, lines 1 and 2) are very similar and characteristic for the A-form of RNA (811 and 1099 cm^{-1}) and C3′-*endo*/*anti* sugar phosphate backbone geometry. The difference spectrum in Fig. 2B, line 3 (three times enlarged), shows bands, assigned to cytosine and adenine, which reflect an intensity increase (ca. 10%) in the spectrum of fMet-$tRNA^{fMet}$ attributable to a structural difference at the 3′-ACC acceptor end of the tRNA caused by the aminoacylation.

3.6. Characterisation of IF2 C·fMet-$tRNA^{fMet}$ and IF2 C-2·fMet-$tRNA^{fMet}$ complexes by Raman spectroscopy

For the spectroscopic analysis of the RNA–protein complexes, the spectra were carefully normalised using two bands, one for the protein and one for the tRNA, considered to be conformation-insensitive: the Phe band at 1003 cm^{-1} and the phosphodiester group band at 1100 cm^{-1}.

The Raman spectrum of the fMet-$tRNA^{fMet}$·IF2 C complex (line 1) and the calculated sum of the component spectra (line 2) are presented in Fig. 3A. Similarly, the spectrum of the fMet-$tRNA^{fMet}$·IF2 C-2 complex (line 1) and the calculated sum of the individual spectra (line 2) are presented in Fig. 3B. As seen from the difference spectra (four times enlarged) between the complexes and the sum of the spectra of their respective components (lines 3 of Fig. 3A,B), the spectral changes occurring upon formation of both complexes are very small. Albeit small, the differences due to complex formation can be appreciated by comparison with the case in which no complex is formed (namely, when either IF2 C or IF2 C-2 is mixed with uncharged initiator tRNA). Thus, the few small spectral differences attributable to formation of the complexes evidenced by the difference spectra (lines 3) are in contrast with the featureless spectra obtained by subtracting the experimental spectra of a mixture of uncharged $tRNA^{fMet}$ and either IF2 C (Fig. 3A, line 4) or IF2 C-2 (Fig. 3B, line 4) from the calculated sum of the spectra of the individual components.

Taken together, the above data indicate that upon complex formation neither the RNA nor the protein moiety undergoes major conformational changes resulting in large spectral changes. Of the small spectral differences caused by complex formation, the most pronounced are seen for the complex between fMet-$tRNA^{fMet}$ and IF2 C-2 (Fig. 3B, line 3). This is likely due to the fact that the size of IF2 C-2 is approximately half that of IF2 C, so that the same fMet-tRNA binding site would encompass a proportionally larger portion of the protein with a consequently larger contribution to the features of the spectrum by the residues directly participating in the interaction. Of the weak difference bands observed (Fig. 3A,B, lines 3), bands at 790 cm^{-1} (cytosine and a contribution from the backbone), at 1315 cm^{-1} (adenine and guanine) and at 815 cm^{-1} (sugar phosphate backbone) can be attributed to the fMet-tRNA moiety of the complex. As to the protein, the spectra do not provide information regarding conformational changes or interactions involving specific amino acid residues.

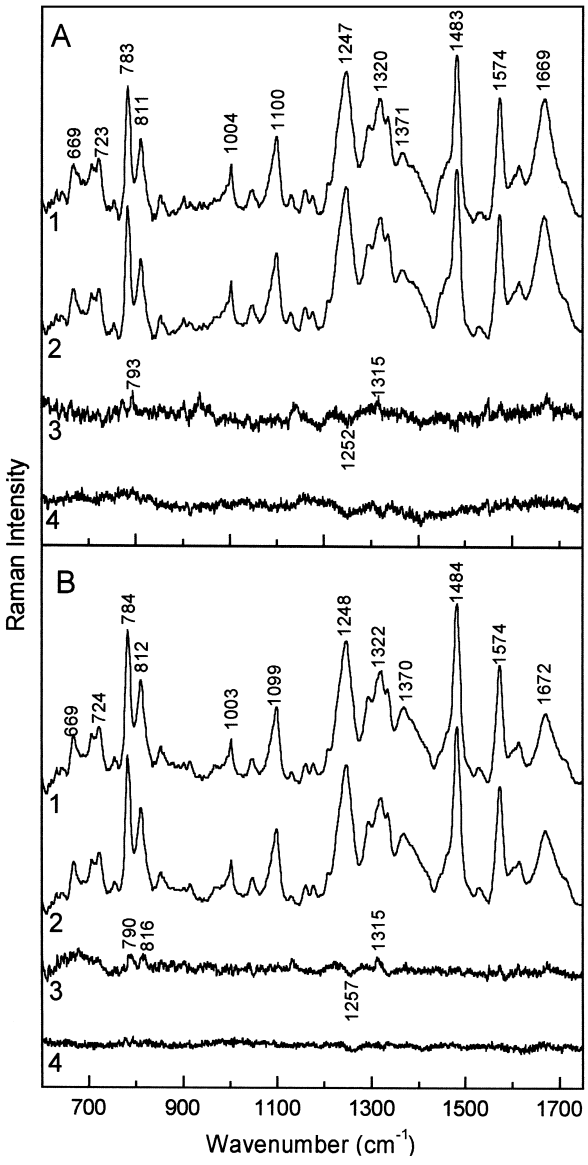

Fig. 3. Raman spectra of the fMet-$tRNA^{fMet}$·IF2 C and fMet-$tRNA^{fMet}$·IF2 C-2 complexes. A: fMet-$tRNA^{fMet}$ complexed with IF2 C (line 1); sum of separately measured spectra of fMet-$tRNA^{fMet}$ and IF2 C (line 2); enlarged (four-fold) difference spectrum between line 1 and line 2 (line 3); enlarged (four-fold) difference spectrum between the spectrum of a mixture of $tRNA^{fMet}$·IF2 C and a calculated sum of the individual spectra of $tRNA^{fMet}$ and IF2 C (line 4). B: fMet-$tRNA^{fMet}$ complexed with IF2 C-2 (line 1); sum of separately measured spectra fMet-$tRNA^{fMet}$ and IF2 C-2 (line 2); enlarged (four-fold) difference spectrum between line 1 and line 2 (line 3); enlarged (four-fold) difference spectrum between the spectrum of a mixture of $tRNA^{fMet}$·IF2 C-2 and a calculated sum of the individual spectra of $tRNA^{fMet}$ and IF2 C-2 (line 4).

Acknowledgements: Financial support from the following grants is gratefully acknowledged: EC-INTAS programme, Italian MURST-CNR Biotechnology Program L. 95/95 and CNR Progetto Strategico (ST74) to C.O.G., EC 'Biotechnology' (BIO4-97-2085) to C.O.G. and U.H., Deutsche Forschungsgemeinschaft (He1318/16, GRK 80/2) to U.H. and H.W., and the Fonds der Chemischen Industrie to U.H. C.O.G. was the recipient of an 'Alexander von Humboldt Forschungspreis'.

References

[1] Gualerzi, C.O. and Pon, C.L. (1990) Biochemistry 29, 5881–5889.
[2] La Teana, A., Pon, C.L. and Gualerzi, C.O. (1996) J. Mol. Biol. 256, 667–675.
[3] Gualerzi, C.O., Severini, M., Spurio, R., La Teana, A. and Pon, C.L. (1991) J. Biol. Chem. 266, 16356–16362.
[4] Spurio, R., Severini, M., La Teana, A., Canonaco, M.A., Pawlik, R.T., Gualerzi, C.O. and Pon, C.L. (1993) in: The Translational Apparatus: Structure, Function, Regulation, Evolution (Nierhaus, K.H., Franceschi, F., Subramanian, A.R., Erdmann, V.A. and Wittmann-Liebold, B., Eds.), pp 241–252, Plenum Press, New York.
[5] Förster, C., Krafft, C., Welfle, H., Gualerzi, C.O. and Heinemann, U. (1999) Acta Crystallogr. D55, 712–716.
[6] Misselwitz, R., Welfle, K., Krafft, C., Gualerzi, C.O. and Welfle, H. (1997) Biochemistry 36, 3170–3178.
[7] Misselwitz, R., Welfle, K., Krafft, C., Welfle, H., Brandi, L., Caserta, E. and Gualerzi, C.O. (1999) FEBS Lett. 459, 332–336.
[8] Spurio, R., Brandi, L., Caserta, E., Pon, C.L., Gualerzi, C.O., Misselwitz, R., Krafft, C., Welfle, K. and Welfle, H. (2000) J. Biol. Chem. 275, 2447–2454.
[9] Dubnoff, J.S. and Maitra, U. (1971) Methods Enzymol. 20, 248–261.
[10] Hirel, P.H., Leveque, F., Mellot, P., Dardel, F., Panvert, M., Mechulam, Y. and Fayat, G. (1988) Biochimie 70, 773–782.
[11] Blanquet, S., Dessen, P. and Kahn, D. (1984) Methods Enzymol. 106, 141–152.
[12] Rodnina, V., Semenko, Y.P. and Wintermeyer, W. (1994) Anal. Biochem. 219, 380–381.
[13] Nesterenko, M.V., Tilley, M. and Upton, S.J. (1994) J. Biochem. Biophys. Methods 28, 239–242.
[14] Ansevin, A.T., Roark, D.E. and Yphantis, D.A. (1970) Anal. Biochem. 34, 237–261.
[15] Yphantis, D.A. (1964) Biochemistry 3, 297–317.
[16] Behlke, J., Ristau, O. and Schönfeld, H.-J. (1997) Biochemistry 36, 5149–5156.
[17] Krafft, C., Hinrichs, W., Orth, P., Saenger, W. and Welfle, H. (1998) Biophys. J. 74, 63–71.
[18] Li, T., Chen, Z., Johnson, E. and Thomas Jr., G.J. (1990) Biochemistry 27, 88–94.
[19] Benevides, J.M., Weiss, M.A. and Thomas Jr., G.J. (1991) Biochemistry 30, 4381–4388.
[20] Sundari, R.M., Stringer, E.A., Schulman, L.H. and Maitra, U. (1976) J. Biol. Chem. 251, 3338–3345.
[21] Majumdar, A., Bose, K.K., Gupta, N.K. and Wahba, A.J. (1976) J. Biol. Chem. 251, 137–140.
[22] Wu, X.-Q. and RajBhandary, U.L. (1997) J. Biol. Chem. 272, 1891–1895.
[23] Spolar, R.S. and Record, M.T.Jr. (1994) Science 263, 777–784.
[24] Meunier, S., Spurio, R. Czisch, M., Wechselberger, R., Guenneugues, M., Gualerzi, C.O, and Boelens, R. (2000) EMBO J., in press.
[25] Peticolas, W.L. (1995) Methods Enzymol. 246, 389–416.